

**Modified method of perturbed stationary states. IV. Electron-capture cross sections for the reaction  $C^{6+} + H(1s) \rightarrow C^{5+}(n,l) + H^+$**

T. A. Green

*Sandia National Laboratories, Albuquerque, New Mexico 87185*

E. J. Shipsey

*Department of Physics, University of Texas at Austin, Austin, Texas 78712*

J. C. Browne

*Departments of Physics and Computer Science, University of Texas at Austin, Austin, Texas 78712*

(Received 14 September 1981)

Previously reported ten-state perturbed stationary-state calculations for  $C^{6+}$ - $H(1s)$  collisions are extended by increasing the basis to include all molecular states correlating to the principal levels  $n=3, 4,$  and  $5$  of the final  $C^{5+}(nlm)$  atomic ion. This allows cross sections to be computed for the angular momentum sublevels,  $l$ , of each of the above  $n$ . The H-atom energy range extends from 13 eV to 27 keV. Adiabatic calculations are done for energies below 1.3 keV, and partially diabatic calculations are done at higher energies. The inclusion of states with magnetic quantum number  $m \geq 2$  in the new basis leads to significant increases in the  $n=5$  capture cross section even at rather low energies. Two translational factors, which depend on the internuclear separation, are employed in the construction of the scattering basis. One is used for the state which correlates to  $H(1s)$ ; the other is used for all states correlating to states of  $C^{5+}$ . For purposes of comparison, cross sections are also computed for the same scattering basis, with the use of the method of Bates and McCarroll and the method of Piacentini and Salin. The heavy-particle motion is treated semiclassically, with the use of Riley's average approximation at energies below 1.3 keV and the straight-line impact-parameter method at higher energies. As in the ten-state calculations, it is shown that adiabatic and diabatic formulations lead to rather different values for the cross sections at the higher energies. The results are compared with the experimental and theoretical cross sections obtained by other researchers.

## I. INTRODUCTION

The presence of highly charged impurity ions in tokamak fusion devices, which also make use of plasma heating by injected neutral hydrogen atoms, has stimulated the use of a variety of experimental and theoretical methods to determine ionization and charge exchange cross sections for collisions of these species.<sup>1</sup> In general, no one technique can cover the required impact energy range from threshold to about 1 MeV/amu. There is, therefore, an unusual opportunity to expand our state of knowledge about heavy particle collisions. One part of the whole picture concerns collisions of completely stripped ions with atomic hydrogen. These systems are special in that the atomic or molecular one-electron wave functions used in theoretical analyses can be known exactly, thus eliminating

one sometimes vexing theoretical uncertainty. In addition, computation for one-electron systems is usually much cheaper, for a given level of accuracy, than is an analogous calculation involving two or more electrons. It is therefore possible to contemplate benchmark close-coupling calculations with large (hopefully nearly converged) basis sets. The resulting cross sections reflect primarily the theory used so the comparison with experiment is of special interest. This paper reports such a calculation for electron capture in  $C^{6+}$ - $H(1s)$  collisions over the energy range from 13 eV/amu to 27 keV/amu. The calculation is based on a theory and a set of related computational techniques described previously.<sup>2-4</sup>

A diagnostic requirement of the magnetic fusion energy program is primarily responsible for the work reported here. This is the need to know the

cross sections for populating the angular momentum sublevels of the upper states of the final atomic ion so that the intensities of the x rays which follow upon capture can be predicted.<sup>5</sup> The ion of primary experimental interest currently is  $O^{8+}$ , and calculations on this system are under way. It was decided, however, to develop the required extensions of our close-coupling scattering program using the  $CH^{6+}$  molecular wave-function data already generated for the cross-section calculations reported in Ref. 4. This allowed us to check the  $l$ -sublevel predictions for  $C^{6+}$  against other theoretical predictions and to study the convergence of the  $C^{6+}$ -H(1s) results as the basis was increased from the ten-states used in Ref. 4 to the 33 states used here. No very large changes in the total capture cross section were expected. This turned out not to be the case, however. Adding new states led to substantial increases in the total capture cross section.

As was the case for the ten-state calculations, the present work is based on a modification of the method of perturbed stationary states which features a new approach to the determination of translational factors.<sup>2,3</sup> In this approach an adiabatic formulation is used at low energies and a partially diabatic formulation is used at high energies. For each formulation the translational factors are determined by approximate Euler-Lagrange optimization.

In order to place our approach into proper perspective, the cross sections obtained from it were compared in Ref. 4 with those obtained using first the theory of Bates and McCarroll<sup>6</sup> and second the theory of Piacentini and Slain.<sup>7</sup> In each case we performed the calculations using the same ten-state molecular basis and a straight-line classical trajectory. Thus the differences in the cross sections reflected only the different theoretical formulations. We have carried out analogous 33-state calculations in the present work. This provides additional insight into the convergence of the three approaches with respect to size of the molecular basis. The calculations are described in Sec. II. The results are presented in Sec. III.

## II. DESCRIPTION OF THE CALCULATIONS

The main calculation, based on Refs. 2–4, is described in Sec. II A. The calculation based on the theory of Bates and McCarroll is described in Sec. II B. The calculation based on the theory of

Piacentini and Salin is described in Sec. II C.

For all these theories, the choice of molecular basis and nonvanishing couplings proceeded along lines suggested by earlier work.<sup>4</sup> Usually, couplings with  $\Delta n \geq 2$  or  $\Delta l \geq 2$  or  $\Delta m \geq 2$  are omitted. (Here the molecular states are labeled with their united-atom quantum numbers  $nlm$ .) The specific choice of basis and couplings for the main high-energy calculation is shown in Table I and the potentials (electronic eigenvalues) for some of these states are shown in Fig. 1. Other calculations referred to in the paper are described in Table II.

### A. The main calculation

With four differences, the calculations were carried out just as described in Ref. 4. The first difference concerns the translational factors introduced into the basis of molecular eigenfunctions. In Ref. 4 different factors were used for each of the most important states correlating to states of  $C^{5+}(nlm)$ . It was found, however, that the ten-state results were not much changed if all these were replaced by their arithmetic mean. Therefore, in order to reduce computer storage and time requirements and thereby go to much larger basis sets, one translational factor was used for the single state correlating to H(1s) and a second one was used for all states correlating to  $C^{5+}(nlm)$ .

The second new aspect of the calculation was the extension of the calculations beyond the maximum internuclear separation,  $R = 20$  a.u., used in Ref. 4 out to  $R = 220$  a.u. At  $R = 220$  a.u., Stark superposition matrices were introduced to obtain the atomic  $n$ ,  $l$ ,  $m$  amplitudes from the molecular ones. The large- $R$  energies and Stark matrices were obtained primarily from the work of Krogdahl.<sup>8</sup> The radial and angular coupling matrix elements for  $R \geq 20$  a.u. were extrapolated continuously from their values computed for  $R = 20$  a.u. All matrix elements which decrease exponentially were extrapolated with the function  $\exp(-R)$ . Within the manifold of states correlating to a given separated-atom principal quantum number  $n$  of  $C^{5+}(nlm)$ , the radial and angular couplings were extrapolated with  $R^{-2}$ . Radial couplings between manifolds were extrapolated with  $R^{-3}$  and angular couplings between manifolds were extrapolated with  $R^{-4}$ . Only the intramanifold couplings are truly important; if the  $l$ -sublevel cross sections were not required, the integrations could be stopped at  $R = 20$  a.u. One aspect of the interac-



tion for  $R \geq 20$  a.u. was entirely neglected. This is the very diabatic avoided crossing between the states 650 and 540 at  $R = 21.36$  a.u. It contributes at most 2% to the capture cross section for an impact velocity  $v = 0.5 \times 10^7$  cm/sec.<sup>9</sup> This velocity corresponds to an H-atom energy of 13.0 eV.

The third change made in the scattering program was to solve the scattering equations only for the initial condition in which the electron is in the H(1s) state, using time-reversal invariance to express the incoming matrix elements in terms of the outgoing ones. In Ref. 4 only the outgoing equations were solved for all initial conditions simultaneously. Evidently, computer memory and computing time are reduced by this change.

The last change made in the scattering program was a simplification of Riley's semiclassical average approximation.<sup>3,4</sup> In this approximation a classical trajectory based on the average molecular potential  $\frac{1}{2}[V_i(R) + V_j(R)]$ , is used for each coupled pair  $ij$  of states in the calculation. Since about 130 state pairs are coupled in the present treatment, and since many of the molecular potentials  $V_i(R)$  lie in rather narrow bands correlating to  $C^{5+}(nlm)$  states of a given  $n$ , it seemed excessive to use so many classical trajectories. The scattering program was revised to let the molecular potential for any given state  $k$  be used for any other state  $p$  in the average potential referred to above. Calculations using from one to nine distinct potentials (45 potential pairs) were possible. Of course, in the calculation of the phase differences, the correct value  $V_i(R)$  was used for each state  $i$ .

The diabatic calculations in this paper were performed with the diabatic transform and the associated translational factors described in Ref. 4. For the adiabatic calculations, the Ref. 4 translational factor for the 540 state was used again for that state and that for the 541 state was used for all the other states. The special matrix element interpolation arrays described in Ref. 4 were, therefore, needed only for about 17 of the 130 matrix elements used in the calculations. The other matrix elements, just as in the approach of Bates and McCarroll, could be calculated by standard methods. Because an optimally chosen translational factor was not used for each state in the scattering expansions, the basis is evidently not optimal in the sense of Ref. 3. The question of optimization was not explored in this paper. On the basis of the study carried out in Ref. 4 and the fact that the linear coefficients in the larger basis are themselves variationally determined, we believe that the

total capture cross section is hardly affected by the two-translational-factor approximation. A somewhat cursory test using Bates-McCarroll factors and some of the other factors from Ref. 4 also indicated that the  $l$ -sublevel cross sections should not be greatly affected by the two-translational-factor approximation.

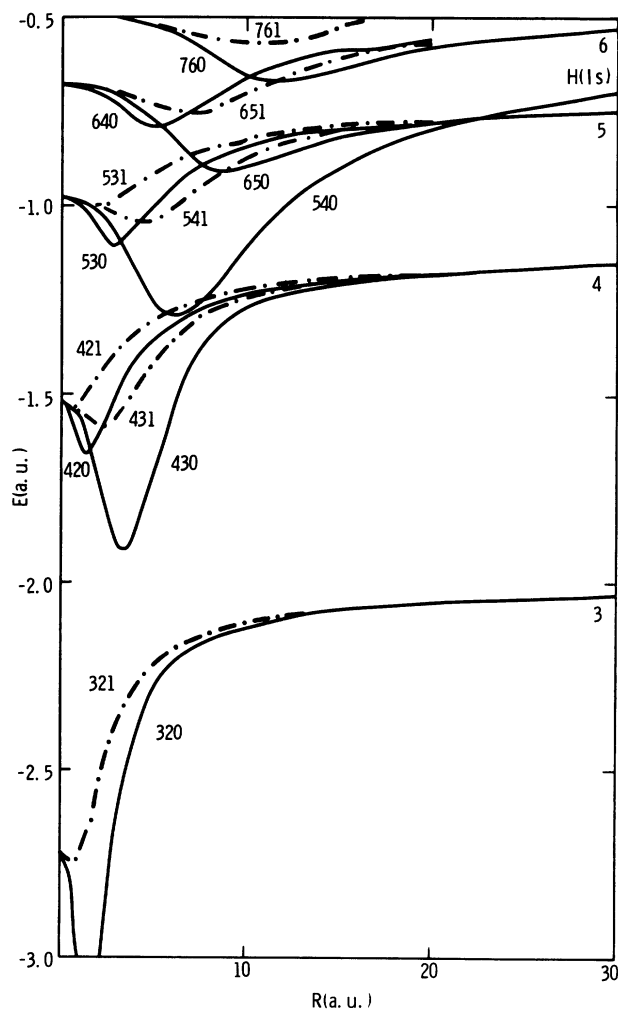


FIG. 1. Electronic energy eigenvalues for  $CH_6^+$ . The curves are labeled by united-atom quantum numbers  $nlm$ . Solid curves are used for  $\Sigma$  states and dashed curves for  $\pi$  states. The separated-atom states H(1s) or  $C^{5+}(n')$  are indicated at the right-hand edge of each curve. Just  $n'$  is used on the graphs for carbon ion states. The initial channel is H(1s); the avoided crossing between states 650 and 540 near  $R = 21.36$  is treated diabatically and the calculations are carried out for  $0 \leq R \leq 20$ . The three most important basis states are 540, 430, and 431.

### B. Calculations based on the theory of Bates and McCarroll

In the theory of Bates and McCarroll,<sup>6</sup> there is one constant translational factor for the molecular states which correlate to separated-atom states of the form  $C^6 + H(nlm)$  and a second constant factor for those which correlate to separated atom states of the form  $C^{5+}(nlm) + H^+$ . In the separated-atom limit, the  $R$ -dependent factors used in the theory described in Sec. II A tend toward those of Bates and McCarroll. The Bates-McCarroll calculation carried out in this paper employs the adiabatic basis described in Table I. It is called calculation number 3 in Table II.

### C. Calculations based on the theory of Piacentini and Salin

In the theory of Piacentini and Salin, the Bates-McCarroll factor for the initial (H atom) state is used for all the states. As a result, no plane-wave translation factors appear in the coupling matrix elements and the net result of the common translational factor is to refer the electron to the H atom. This is calculation 4 of Table II.

## III. RESULTS

As explained in the Introduction, the main results consist of cross sections  $Q_n$  for electron capture into the principal  $n$  manifolds of  $C^{5+}(n, l, m)$

and  $l$ -sublevel capture probabilities  $P_l$  for each  $n$ . These were obtained by the method described in Sec. II A and will be presented first. Then, comparisons will be made among cross sections  $Q_n$  obtained from several versions of the method described in Sec. II A and cross sections obtained using the method of Bates and McCarroll (Sec. II B) and Piacentini and Salin (Sec. II C).

Table III contains the main results. These were obtained with calculations 1, 6, and 7 of Table II. The total capture cross section can be obtained by adding up the  $Q_n$ . Capture to the  $n=4$  manifold is the most important contribution at all energies. However, capture to  $n=5$ , which is not mediated by an avoided crossing such as that shown in Fig. 1 for the states 540 and 430, contributes from 10 to 30% of the total cross section at velocities  $v$  above  $1 \times 10^7$  cm/sec. This velocity range corresponds to H-atom laboratory energies above 52 eV, as can be deduced from the velocity and energy columns of Table IV. Capture to the  $n=3$  manifold contributes about 5% of the cross section at the higher energies and is negligible at the lower energies. The cross section for  $n \geq 6$  is an estimate based on the six states shown in Table I. From the fact that at  $v = 22.8 \times 10^7$  cm/sec  $Q_5$  increased from about six to about  $12 \times 10^{-16}$  cm<sup>2</sup> when the basis was increased from ten to 33 states, we estimate that the analogous inclusion of additional states for  $n \geq 6$  could double the values of  $Q_n \geq 6$  in Tables III and IV.

Except for  $n=3$ , the cross sections in Table III are for the most part larger than those shown in

TABLE II. Brief description of the various calculations for which results are presented in Tables III and IV and Fig. 1.

Calculation number	No. of states	Expansion type	Translation factors <sup>a</sup>	Further description
1	33	diabatic <sup>b</sup>	diabatic <sup>b</sup>	See Table I
2	33	adiabatic	adiabatic <sup>c</sup>	See Table I
3	33	adiabatic	Bates-McCarroll	See Table I
4	33	adiabatic	Piacentini-Salin	See Table I
5	24	diabatic	diabatic	Top two $l$ s only for $n=4$ and $n=5$
6	33	diabatic	diabatic	States 11–14 out of Table I; rest of $n=3$ in.
7	26	adiabatic	adiabatic	$n=4$ and $n=5 + 650$

<sup>a</sup>There is one factor for the 540 state which alone correlates to H(1s) and one common factor for all the carbon-correlating states.

<sup>b</sup>See Fig. 5 of III.

<sup>c</sup>For 540 see Fig. 4 of III; the 541 factor from the same figure was used for all the other states.

Table III of Ref. 4, where just the first ten states of Table I were used. The  $n=4$  cross section is either decreased very slightly or increased by amounts up to about 10%. The  $n=5$  cross section is about doubled at all energies except the lowest. By contrast, the cross section for  $n=3$  is reduced at high energy. Finally, the inclusion of states 760, 761, 640, and 641 in the present calculation lead to a substantial increase in the cross section for  $n \geq 6$ . The increases just described cause the total capture cross section to increase by from 10 to 30% relative to the ten-state results of Ref. 4. This is

shown in Fig. 2. Studies at  $v=22.8 \times 10^7$  cm/sec showed that states with magnetic quantum number  $m \geq 2$  are primarily responsible for the  $n=5$  cross-section increase.

The total capture cross section agrees closely with the experimental cross section for the reaction  $O^{6+} + H \rightarrow O^{5+} + H^+$  at high energy, where  $C^{6+}$  and  $O^{6+}$  should have nearly equal capture cross sections.<sup>10</sup> At  $v=2 \times 10^7$  cm/sec the total cross section of  $21 \times 10^{-16}$  cm<sup>2</sup> is in rather good agreement with the experimental value  $17.8 \pm 6.3 \times 10^{-16}$  cm<sup>2</sup> obtained for  $C^{6+}$  by Phaneuf<sup>11</sup> at  $v=2.06 \times 10^7$

TABLE III. Computed  $n$ -manifold sections  $Q_n$  and relative  $l$ -sublevel probabilities  $P_l$  for capture into states  $nlm$  of  $C^{5+}$ .

Velocity <sup>a</sup>	Calculation <sup>b</sup>	$n^c$	$Q_n^d$	$P_o^e$	$P_1$	$P_2$	$P_3$	$P_4$
0.5	7	5	0.00					
		4	0.47	0.135	0.100	0.357	0.408	
1.0	7	5	0.39	0.099	0.161	0.259	0.339	0.143
		4	3.82	0.113	0.305	0.325	0.257	
1.6	7	5	3.28	0.080	0.091	0.152	0.353	0.324
		4	10.99	0.082	0.216	0.261	0.441	
2.0	7	5	4.80	0.100	0.139	0.174	0.297	0.289
		4	16.19	0.072	0.205	0.200	0.523	
3.5	7	5	6.45	0.101	0.139	0.288	0.320	0.152
		4	29.86	0.062	0.193	0.338	0.407	
5.0	1	$\geq 6$	0.17					
		5	6.62	0.143	0.292	0.288	0.195	0.081
		4	37.44	0.064	0.224	0.356	0.355	
		3	0.02 <sup>3</sup>	0.229	0.463	0.308		
7.5	1	$\geq 6$	0.52					
		5	7.76	0.040	0.146	0.197	0.286	0.331
		4	38.08	0.058	0.198	0.381	0.364	
10.0	1	$\geq 6$	0.64					
		5	9.47	0.025	0.070	0.135	0.311	0.458
		4	36.61	0.050	0.189	0.381	0.380	
		3	1.07	0.271	0.470	0.259		
15.0	1	$\geq 6$	2.28					
		5	12.52	0.014	0.040	0.103	0.247	0.595
		4	28.99	0.033	0.130	0.298	0.539	
		3	2.13	0.162	0.437	0.400		
20.0	1	$\geq 6$	2.87					
		5	12.20	0.011	0.045	0.108	0.245	0.591
		4	23.41	0.028	0.104	0.304	0.565	
		3	2.24	0.106	0.333	0.561		
22.8	1	$\geq 6$	2.58					
		5	12.29	0.013	0.054	0.105	0.238	0.590
		4	20.26	0.023	0.091	0.305	0.580	
		3	1.96	0.085	0.289	0.626		

<sup>a</sup>Impact velocity in units of  $10^7$  cm/sec.

<sup>b</sup>Defined in Table II.

<sup>c</sup>Principal quantum number of  $C^{5+}(nlm)$ .

<sup>d</sup>Cross sections in units of  $10^{-16}$  cm<sup>2</sup>.

<sup>e</sup> $l$ -sublevel population probability sums to unity.

TABLE IV. Comparison of the capture cross sections  $Q_n$  resulting from the calculations described in Table II.

Velocity <sup>a</sup>	H laboratory energy <sup>b</sup>	Calculation number <sup>c</sup>	$Q_3^d$	$Q_4$	$Q_5$	$Q_6$	$Q_{tot}^e$
5.0	1.30	1	0.02	37.44	6.62	0.17	44.25
		6	0.02	37.38	6.72	0.02	44.14
		2	0.02	37.16	6.67	0.15	44.00
		3	0.02	38.04	7.05	0.14	45.25
7.5	2.94	4					46.29
		1	0.21	38.08	7.76	0.52	46.57
		2	0.20	37.76	7.78	0.49	46.23
		3	0.22	39.58	7.82	0.38	48.00
10.0	5.22	4					46.79
		1	1.00	36.61	9.47	0.64	47.71
		6	1.07	36.72	9.70	0.08	47.57
		5	1.00	37.02	8.89	0.70	47.61
15.0	11.74	2	0.94	35.73	10.37	0.72	47.77
		3	0.99	37.22	11.06	0.48	49.76
		4					46.34
		1	2.19	28.99	12.52	2.28	45.97
20.0	20.88	6	2.13	29.50	13.38	0.13	45.13
		2	1.83	27.62	17.38	2.52	49.35
		3	1.36	35.24	11.23	3.61	51.44
		4					46.51
22.8	27.08	1	1.95	23.41	12.20	2.87	40.43
		6	2.24	23.28	13.67	0.24	39.43
		2	1.56	22.23	20.48	3.45	47.82
		3	1.13	30.43	12.83	4.13	48.53
22.8	27.08	4					42.61
		1	1.69	20.26	12.29	2.58	36.82
		6	1.96	20.12	14.05	0.26	36.39
		5	1.82	20.27	11.65	2.68	36.43
22.8	27.08	2	1.31	19.82	21.62	3.36	46.11
		3	1.10	26.14	13.48	4.62	45.34
		4					39.86

<sup>a</sup>In units of  $10^7$  cm/sec.

<sup>b</sup>In units of keV.

<sup>c</sup>See Table II.

<sup>d</sup>All cross sections in units of  $10^{-16}$  cm<sup>2</sup>.

<sup>e</sup>The total electron capture cross section.

cm/sec. At  $v = 1.6 \times 10^7$  cm/sec the total cross sections of  $14.3 \times 10^{-16}$  cm<sup>2</sup> exceeds by an uncomfortable amount Phaneuf's experimental value  $7 \pm 5.6 \times 10^{-16}$  cm<sup>2</sup>, obtained at  $v = 1.66 \times 10^7$  cm/sec.

Figure 3 compares the  $l$ -sublevel capture probabilities for  $v = 22.8 \times 10^7$  cm/sec with the  $v = 21.9 \times 10^7$  cm/sec classical trajectory Monte Carlo results of Olson<sup>12</sup> and with the high-velocity-limit values of Abramov *et al.*<sup>13</sup> Also shown is the statistical straight line proportional to  $2l + 1$ . Our results agree quite well with those of Olson and predict a fairly strong trend toward the

population of the highest  $l$  value at the expense of the lowest ones.

The results of the comparative studies are presented in Table IV, Fig. 2, and Fig. 4. Table IV documents a number of interesting points about high-energy calculations of different types. The comparison of calculations 1 and 6 shows that states numbered 11–14 in Table I are very important for  $Q_6$  ( $\equiv Q_n$ ,  $n \geq 6$ ), that the states 320 and 321 are nearly sufficient by themselves for  $Q_3$ , and that the cross sections  $Q_4$ ,  $Q_5$ , and  $Q_{tot}$  are not much influenced by the changes involved in going from calculation 1 to calculation 6. Calculations 1

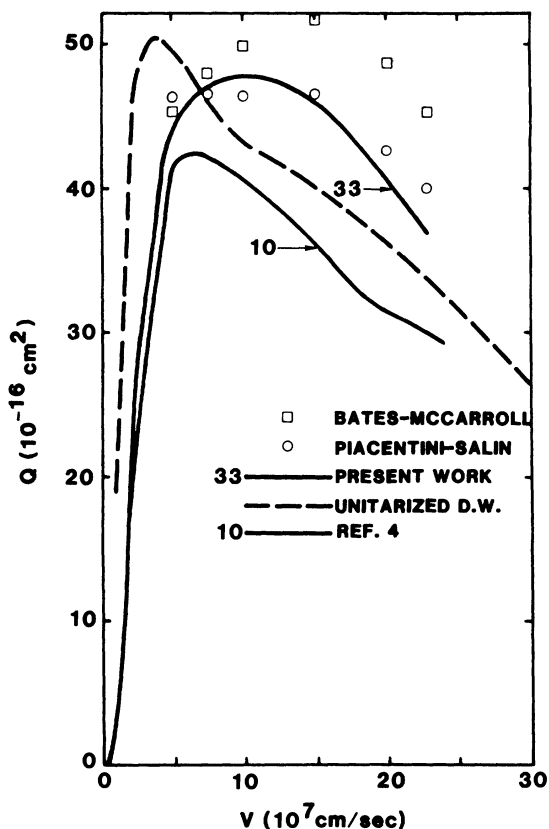


FIG. 2. Total capture cross section  $Q$ . The solid lines represent the ten-state calculation of Ref. 4 and the 33-state calculation from the present work. The squares represent a 33-state adiabatic Bates-McCarroll calculation from the present work. The circles represent a 33-state Piacentini and Salin calculation from the present work. The dashed curve represents the unitarized distorted-wave calculation of Ryufuku and Watanabe. The upper solid curve was smoothed slightly. It departs by small amounts ( $<1\%$ ) from several of the data points in Table IV.

and 6 were done separately because we did not find a convenient way to include all the states in a single calculation simultaneously.

Calculation 5 was done to see if the lower  $l$  values could be safely omitted, in order to make the calculations cheaper. The results at  $v=10$  and  $v=22.8$  show that this is indeed the case. However, it was found that the  $P_l$  obtained from calculation 5 are not good approximations to those obtained from calculation 1.

The rest of the calculations are done in the adiabatic formulation, using the expansion defined in Table I. The  $Q_{\text{tot}}$  column and Fig. 2 show that the trend exhibited in Fig. 6 of Ref. 4 is found once again in the present better-converged calculations.

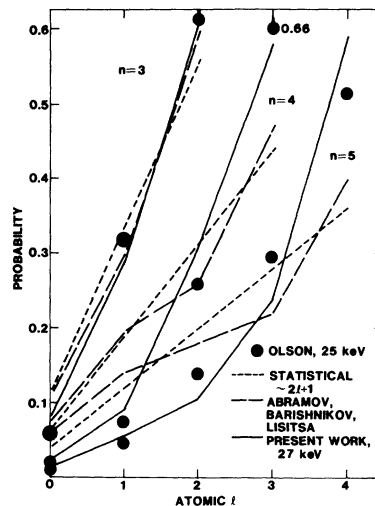


FIG. 3.  $C^{5+}(nl)$  atomic  $l$ -subshell occupation probabilities. The results of this work (solid line) are for 27 keV/amu; the results of Olson are for 25 keV/amu; the results of Abramov *et al.* are a high velocity limit; the statistical result is proportional to  $2l+1$ .

Consider first calculations 1, 2, and 3. At the lower velocities adiabatic and diabatic formulations agree to about 3%. As the velocity is increased, the adiabatic formulation leads to cross sections

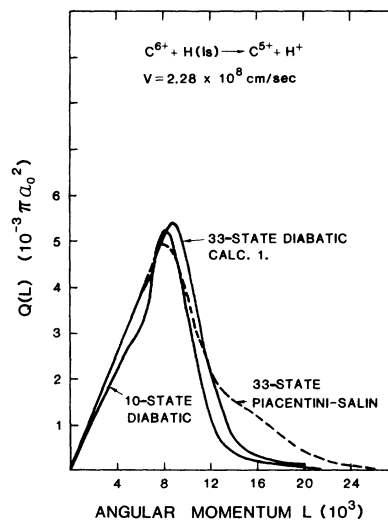


FIG. 4. Total capture cross section  $Q(L)$  vs partial wave  $L$ . The ten-state result is taken from Ref. 4 and shows the  $L$  regions most influenced by the larger basis. The Piacentini-Salin curve illustrates its peculiar high-energy character. The straight line for  $L < 8000$  corresponds to nearly unit capture probability. This demonstrates clearly that the use of weak coupling methods for  $L < 10000$  is open to serious question. The Olson and Salop absorbing sphere model, however, would be appropriate for use at this energy.



which exceed that of the diabatic formulation by about 20%. The 20% differences should be well in excess of the modification of the cross sections which could result from the use of a larger basis. Thus, we find that adiabatic and diabatic formulations are not equivalent at high energy. The weak coupling approximation used in Ref. 3 as the basis for Euler-Lagrange optimization of the translational factors requires us to use only the diabatic representation at high energy. However, it is plausible on first principles that a diabatic formulation should be preferred in the present circumstances. The two-state diabatic transform between states 540 and 430 (see Fig. 5 of Ref. 3) produces one hydrogenlike state and one carbonlike state, and associates appropriate translation factors with them, down to an internuclear separation of about 7 a.u. Inside of this internuclear separation both states begin to delocalize and ultimately transform into molecular states. Given that an atomic basis expansion should be a good one at high energies, the diabatic formulations's capacity to produce a more hydrogenlike initial basis state suggests that this formulation is to be preferred over an adiabatic one. It will be interesting to see what happens for other systems.

The difference shown in Table IV between calculations 2 and 3 is entirely due to the use of the translational factors of Ref. 4 for calculation 2 and those of Bates and McCarrroll for calculation 3. It is interesting that while the total cross sections agree rather closely, the distribution of the cross section between levels 4 and 5 is quite different. It will take rather sophisticated experimentation<sup>5</sup> to study the charge exchange process in this much detail.

Let us now consider calculation 4. It is done using the method of Piacentini and Salin (PS) as described in Sec. II C. For this theory, adiabatic and diabatic formulations yield the same total cross sections. Since the carbon states effectively have the wrong translational factor, and are not channel states asymptotically, we can only obtain the total capture cross section. With a ten-state basis, the PS cross section was nearly equal to that obtained from the method of Bates and McCarrroll. This time, at high energy, the PS cross section lies below that of Bates and McCarrroll and somewhat above the diabatic result obtained in calculation 1. This behavior is shown in Fig. 2.

Table IV together with Table II of Ref. 4 allows one to consider the convergence of the PS method

for three, ten, and 33 states. While the convergence is nonuniform with respect to basis size and velocity, it is quite remarkable that the three and 33 states expansions agree to better than 15% at all energies. Since Salop and Olson<sup>14</sup> showed that their three- and six-state PS results for  $C^{6+}$ -H collisions agree rather closely with each other, it follows that their six-state total cross sections<sup>14</sup> are in close agreement with the results of both calculations 4 and 1 as given in Tables III and IV. It is impressive how rapidly the PS expansion converges in this system. In a crude sense, this may occur because the effective omission of translational factors allows each PS state to overlap a number of true channel states, so that the Hilbert space needed for the collision is better covered by just a few such states. Besides rapid convergence, the PS approach has another interesting feature at high energy. This is shown in Fig. 4, which gives the dependence of the cross section upon the impact angular momentum  $L$ . The PS formulation does not treat the distant collisions very accurately. All of the calculations with appropriate translational factors lead to essentially the same curve at large  $L$  as that shown for calculation 1.

Figure 3 exhibits two other interesting points. The first is the region of  $L$  where the ten and 33-state diabatic calculations differ. It is seen that the additional states extend the effective range of the  $C^{6+}$ -H interaction significantly. The other point is the linear dependence of  $Q(L)$  out to  $L = 8000\hbar$ . This line corresponds to a capture probability of about 0.99. Thus the absorbing sphere model introduced by Olson and Salop<sup>15</sup> for use at the cross-section maximum appears to be valid at  $v = 22.8 \times 10^7$  cm/sec. The corresponding graphs for  $v = 5 \times 10^7$  cm/sec and  $15 \times 10^7$  cm/sec show that the absorbing sphere model is also justified at the higher velocity. However, at  $v = 5 \times 10^7$  cm/sec  $Q(L)$  oscillates with  $L$  and falls significantly below the unit probability curve over much of the important range of  $L$ . Note, that the character of  $Q(L)$  shown in Fig. 3 suggests that a good large- $L$  calculation alone would be sufficient to obtain a reliable total cross section.

As stated in Ref. 4 our ten-state results were not in very good agreement with those of Vaaben and Briggs,<sup>16</sup> Bottcher,<sup>17</sup> and Abramov *et al.*<sup>18</sup> The disagreement is more marked for the present calculations. However, it is worth pointing out the results of Ref. 18 apply only to the  $n = 4$  level, and that for this level the agreement is rather good at the higher energies. Finally, Fig. 2 shows that our

33-state calculation lies above the unitarized distorted-wave result of Ryufuku and Watanabe<sup>19</sup> at high energy.

#### ACKNOWLEDGMENTS

We wish to acknowledge conversations and correspondence with R. E. Olson, R. A. Phaneuf, and R. C. Eisler, all of whom have provided un-

published information and data relevant to this work. We also want to thank J. M. Peek, M. E. Riley, W. Thorson, T. Winter, J. Vaaben, and C. Bottcher for very helpful discussions. This work was supported in part by the Office of Magnetic Fusion Energy. It was also supported in part by the Office of Naval Research under Contract No. N000-14-67-A-0126-0017 and by the Robert A. Welch Foundation Grant No. F-379.

<sup>1</sup>R. E. Olson, in *Proceedings of the International Conference on the Physics of Electronic and Atomic Collisions, 1979, Kyoto*, edited by N. Oda and K. Takayanagi (The Society for Atomic Collision Research, Kyoto, 1979).

<sup>2</sup>T. A. Green, *Phys. Rev. A* **23**, 519 (1981). This paper describes the method used here in relation to other theoretical approaches.

<sup>3</sup>T. A. Green, *Phys. Rev. A* **23**, 532 (1981).

<sup>4</sup>T. A. Green, E. J. Shipsey, and J. C. Browne, *Phys. Rev. A* **23**, 546 (1981).

<sup>5</sup>R. C. Eisler, *Phys. Rev. Lett.* **38**, 1359 (1977).

<sup>6</sup>D. R. Bates and R. McCarroll, *Proc. Soc. (London)* **A245**, 175 (1958).

<sup>7</sup>R. D. Piacentini and A. Salin, *J. Phys. B* **7**, 1666 (1974).

<sup>8</sup>M. K. Krogdahl, *Ap. J.* **100**, 311 (1945). Also see K. Omidar, *Phys. Rev.* **153**, 121 (1967).

<sup>9</sup>The study upon which this result is based will be reported in the near future.

<sup>10</sup>D. H. Crandall, R. A. Phaneuf, and F. W. Meyer, *Phys. Rev. A* **19**, 504 (1978).

<sup>11</sup>R. A. Phaneuf, *Phys. Rev. A* **24**, 1138 (1981). We are indebted to Dr. Phaneuf for information about these measurements in advance of publication.

<sup>12</sup>R. E. Olson, private communication.

<sup>13</sup>V. A. Abramov, F. F. Baryshnikov, and V. S. Lisitsa, *Pisma Zh. Eksp. Teor. Fiz.* **27**, 494 (1978) [*JETP Lett.* **27**, 464 (1978)].

<sup>14</sup>A. Salop and R. E. Olson, *Phys. Rev. A* **16**, 1811 (1977).

<sup>15</sup>R. E. Olson and A. Salop, *Phys. Rev. A* **14**, 579 (1976).

<sup>16</sup>J. Vaaben and J. S. Briggs, *J. Phys. B* **10**, L521 (1977).

<sup>17</sup>C. Bottcher, *J. Phys. B* **10**, L213 (1977).

<sup>18</sup>V. A. Abramov, F. F. Baryshnikov, and V. S. Lisitsa, *Zh. Eksp. Teor. Fiz.* **74**, 897 [*Sov. Phys.—JETP* **47**, 469 (1978)].

<sup>19</sup>R. Ryufuku and T. Watanabe, *Phys. Rev. A* **19**, 1538 (1979).